

Absorption of Low-Energy UV Radiation by Human Telomere G-Quadruplexes Generates Long-Lived Guanine Radical Cations

Akos Banyasz^a, Lara Martínez-Fernández^b, Clémence Balty^a, Marion Perron^a, Thierry Douki^c, Roberto Improta^{a, b} * and Dimitra Markovitsi^a *

^a LIDYL, CEA, CNRS, Université Paris-Saclay, F-91191 Gif-sur-Yvette, France

^b Istituto Biostrutture e Bioimmagini- Consiglio Nazionale delle Ricerche, Via Mezzocannone 16, I-80134 Napoli, Italy

^c CEA, INAC-SyMMES Laboratoire des Lésions des Acides Nucléiques, F-38000 Grenoble, France.

Supporting Information

- **Experimental absorption spectra of monomeric guanine radicals**
- **Fitting of transient absorption signals**
- **Computational details and additional results**

Experimental absorption spectra of monomeric guanine radicals

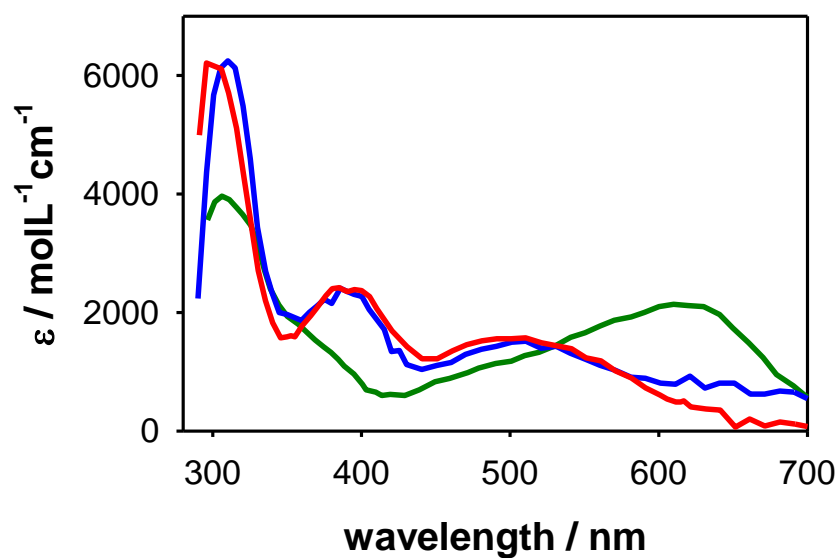


Figure S1. Experimental absorption spectra of monomeric guanine radicals. Radical cation ($\text{G}^{\bullet+}$) (red), deprotonated (G-H1^{\bullet}) radical (blue) and deprotonated (G-H2^{\bullet}) radical (green). From the 1989 study by Candeias and Steenken.¹

Fitting of the transient absorption signals

Fits of the transient signals were performed for those recorded on the visible domain where final photoproducts and possible reaction intermediates do not absorb.

First we fitted signals recorded between 5 and 180 ms because the transient spectra in Figure 3c indicate that after 5 ms the dominant species are (G-H1)· radicals. After 180 ms, decays are not reliable; due to the flow of the solution, the transient species quit the probed volume. This has been checked by recording the transient signal of thymine single strands at 285 nm. At this wavelength, a constant negative value, correlated with the CPD formation, is expected² (Figure S2).

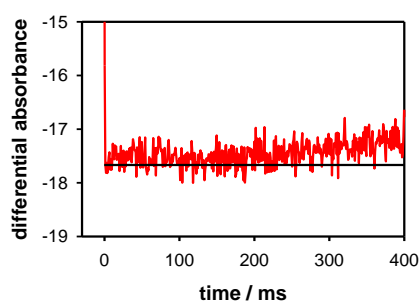


Figure S2. Red: transient signal obtained for the single strand of (dT)₂₀ at 285 nm following excitation at 266 nm. Deviation from horizontality (black) is due to flowing of solution.

In order to get an insight on the dynamics corresponding to the spectra evolution observed for TEL21/Na⁺ between 0.1 and 5 ms (Figure 6), we fitted the decays on this time range using mono-exponential functions $\Delta A_0 \cdot \exp(-t/\tau) + C$. The time constants obtained for several independent experiments fall in the range 1.0-1.4 ms, without showing a particular wavelength dependence. The reproducibility of these signals is shown in Figure S3.

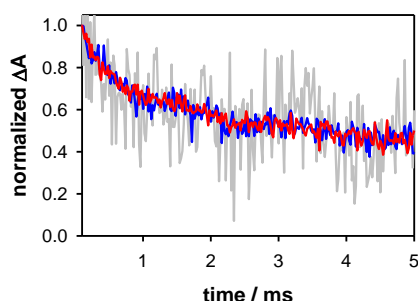


Figure S3. Transient absorption signals recorded for G4 at 550 nm for excitation intensities 0.7 (grey), 1.5 (blue) and 2 (red) MWcm⁻¹, leading to ratios of one- versus two-photon ionization of 1.5, 0.75 and 0.52, respectively.

Computational details and additional results

1. Computational Details

1.1 Geometry optimizations

Guanine Monomer (G). Unless specified, we used 9-methylguanine (G) as model for the monomer calculations. The ground state minima of the neutral (G), radical cation (G)⁺ and deprotonated radicals, (G-H1)[•] and (G-H2)[•], were optimized by means of calculations rooted in the Density Functional Theory (DFT) using the M052X³⁻⁴ functional and the 6-31G(d) basis set. These functional and basis set were selected in order to be consistent with the level of theory used for G-quadruplex calculations (see below). Solvent effects were included by the Polarizable Continuum Model (PCM)⁵⁻⁶ and, in some cases, also by including 5 explicit water molecules (Figure S4a).

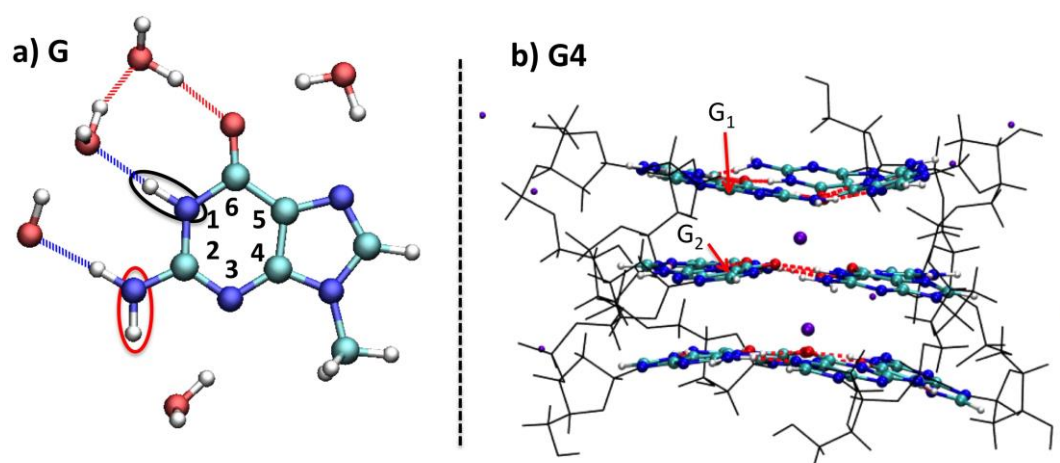


Figure S4. Schematic drawing of the different systems under study; 9-methylguanine, G (see atom labels) and three guanine antiparallel tetramers G4 (QM part in tubes and MM in lines). The proton framed in black is missing in the deprotonated (G-H1)[•] radical and that framed in red in the deprotonated (G-H2)[•] radical.

G-Quadruplex (G4). Due to the large size of the system under study (Figure S4b) we resorted to a mixed Quantum Mechanical/Molecular Mechanics (QM/MM) approach for the geometry optimization of the ground state minima of G4, (G4)⁺, (G4-H1)[•] and (G4-H2)[•]. The 12-guanine bases plus the inner Na⁺ cations were described at the QM level, whereas the phospho-deoxyribose backbone and the remaining Na⁺ cations were treated at the MM level. The M052X/6-31G(d) level of theory was selected for the QM calculations and the Amber parm96.dat⁷ parameter were used for the MM calculations (using the ONIOM⁸

interface as implemented in Gaussian09⁹). The M052X functional was selected since it provides accurate results for stacked systems as the one here considered, due to the inclusion of specific treatments for dispersion interactions⁶. Since in the tetrads most of the hydrogen bond (HB) donor/acceptor moieties are involved in the HB network stabilizing the quadruplex, here we included only bulk solvent effects by PCM.

1.2 Absorption spectra

Guanine monomer (G). At the ground state optimized minima, we computed the vertical absorption energies (VAE) of the 20 lowest energy excited states of the radicals $(G)^+$, $(G-H1)^\cdot$ and $(G-H2)^\cdot$; 4 excited states were computed for G (all those with VAE < 6.5eV). The time-dependent extension of DFT (TD-DFT) was used, selecting also in this case the M052X functional. The basis set for the VAE calculation in the monomer was increased from 6-31G(d) up to 6-31+G(d,p). A detailed analysis of the effect that the basis set extension has on the VAE can be found in section 2.2.

G-Quadruplex (G4). The same procedure was followed to compute the VAE of G4 but in this case the size of the system limited the basis set to 6-31G(d). The number of computed excited states is 60 for G4, 140 for $G4^+$ and 120 for the $(G4-H1)^\cdot$ and $(G4-H2)^\cdot$. In order to cover the blue region of the experimental spectra it was necessary to limit the number of guanine bases in the QM region to 8 bases instead of 12. However, we have checked that the main features of the absorption spectra were not affected by this approximation (Figure 10)

Spectra simulation: Each VAE was shifted by -0.6 eV. This value is selected to superimpose the computed (at this level of theory) and the experimental spectra of dG in water. It is clear, however, that we do not expect that different sources of errors in our calculations (functional, incomplete basis set, lack of vibronic and thermal effects) would need the same corrections for all the species considered. As a consequence, relative errors of 0.1/0.2 eV are well within the expected accuracy of any computational approach used on such large systems. For easier comparison with the experimental spectra each transition was convoluted with a Gaussian with half width half maximum of 0.3 eV.

1.3 H1 and H2 deprotonation energies

In order to estimate the relative stability of the two neutral radicals (G-H1) \cdot and (G-H2) \cdot , single point calculations on top of the optimized M052X/6-31G(d) geometries were performed extending the basis set for the monomer (Table S1). For all of them, (G-H1) \cdot is more stable (0.4-3.7 kcal/mol) than (G-H2) \cdot . In case of G4, the H2 is more stable (~3kcal) using the 6-31G(d) basis set and the calculations for the monomer show that an increase of basis set does not revert the relative stability of the two radicals.

Table S1. Energies (a.u.) of the radical species (G-H1) \cdot and (G-H2) \cdot optimized at the PCM-M052X/6-31G(d) level of theory and calculated with the M052X functional combined with different basis set for the guanine monomer (G) without and with explicit water molecules and for the quadruplex (G4). The electronic energy difference between the two tautomers is reported in the last column.

	(G-H1) \cdot	(G-H2) \cdot	ΔE (kcal)
G+PCM			
6-31G(d)	-581.171950402	-581.171297687	0.40
6-31+G(d,p)	-581.208680706	-581.206369544	1.45
6-311+G(2d,2p)	-581.359547889	-581.356990792	1.60
G+5H₂O+PCM			
6-31G(d)	-963.257871619	-963.252054095	3.65
6-31+G(d,p)	-963.385838932	-963.381075111	2.98
6-311+G(2d,2p)	-963.670555314	-963.665430627	3.21
G4+PCM			
6-31G(d)	-6834.45467239	-6834.45936933	-2.94

2. Computational Results

2.1. Spectra

In Figure S5 we compare our computed VAE for the monomer G with the experimental spectra extracted from reference 1. The computed spectra are in good agreement with the experimental ones. More precisely, our calculations predict three main intense transitions for both for (G) $^+$ (peaking at 300, 400 and ~500 nm) and (G-H1) \cdot (peaking at 310, 400 and 580 nm). For (G-H1) \cdot , the first and third transitions are less intense and red-shifted compared to (G) $^+$ (significantly in the case of the third band). Our calculations probably underestimate the intensity of the 310 peak of (G-H1) \cdot , which, however, is correctly

predicted to be red-shifted with respect to the maximum of $(G)^+$. For the alternative deprotonated radical $(G-H2)^\bullet$ our calculations predict a main intense transition at ~ 680 nm, and two less intense at 310 and 390 nm. The lowest-energy peak is red-shifted with respect to the experimental one (~ 620 nm). However, this error is smaller than 0.2 eV on the energy scale and could simply arise from the use of a uniform shift of 0.6 eV for all the species (see computational details).

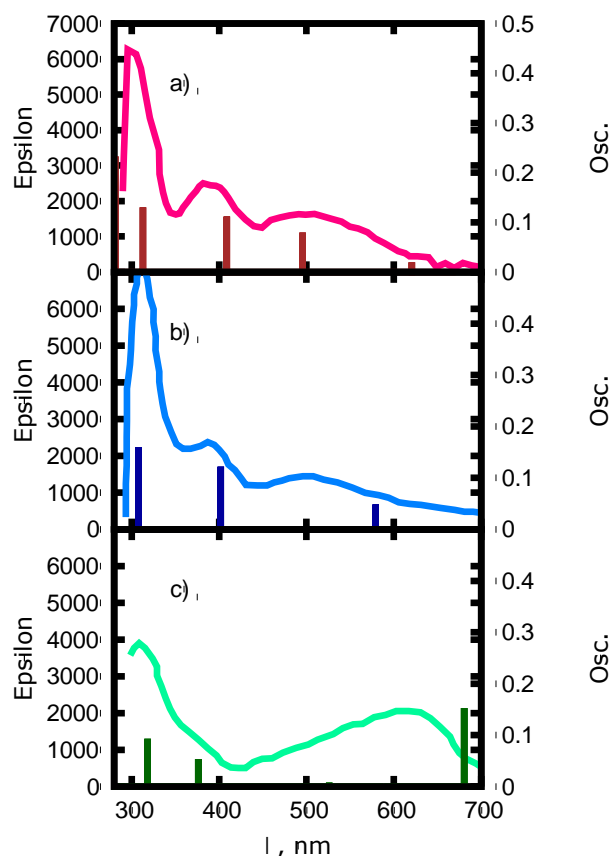


Figure S5. Calculated VAE of G^+ (a), $(G-H1)^\bullet$ (b) and $(G-H2)^\bullet$ (c) in sticks compared with experimental spectra¹, calculated at the PCM+5H₂O/TD-M052x/6-31+G(d,p)//M052x/6-31G(d) level of theory. All VAE are shifted by 0.6 eV.

In order to compare the differences between the radical absorption spectra of G and G4, it is necessary to compute the spectra at the same level of theory using similar approaches. We have thus re-optimized and computed the spectrum of the guanine base (i.e. without a methyl group in position 9), since this is the compound treated at the QM level in G4), and including solvent effects by PCM only (i.e. without explicitly considering solvent molecules). In Figure S6 we report the spectra of the different isolated radicals with those computed within G4. The spectra are rather similar, indicating that the inclusion of the radical species into G4 does not significantly affect the position of the band maxima, but for an additional

red-shift of the peak at 680 nm. However, the effect on the band maximum is rather modest on the energy scale, i.e. the band maximum of the red-shifted peak of (G-H2) \cdot decreases by only 0.15 eV in G4. The most important differences between the G and G4 radical spectra concern the relative intensities of the different absorption features (Figure S6). 1) Both (G4) $^+$ \cdot and, especially, (G4-H1) \cdot exhibit a larger absorption in the red wing, for $\lambda > 800$ nm and 2) The relative intensity of the feature at 500-550 nm for (G4-H1) \cdot and (G) $^+$ \cdot increases, whereas at ~ 400 nm both decrease, this effect being particularly pronounced for (G) $^+$ \cdot . For the monomer, the peak at ~ 400 nm is significantly more intense than that at ~ 550 nm while in G4 these two features have similar intensities. This difference is due to a partial localization of the positive charges over several bases between G $^+$ and another guanine in the stacked tetramer (see G $_1$ and G $_2$ in Figure S4b) with Mulliken charges 0.86 and 0.14 a.u., respectively.

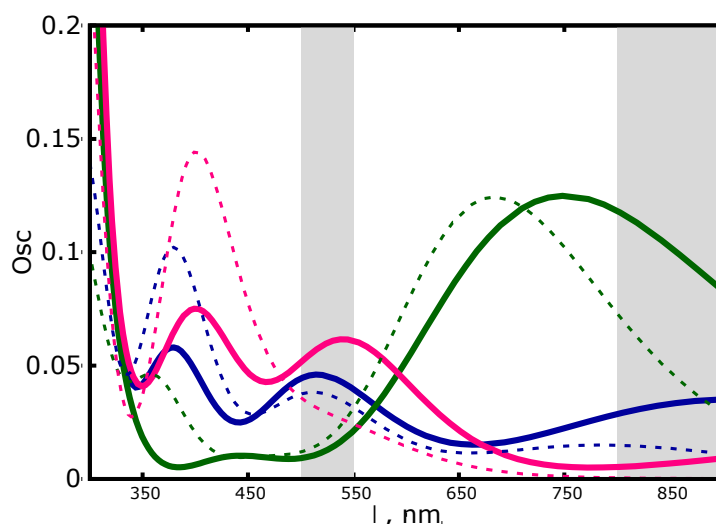


Figure S6. Simulated absorption spectra of G4 $^+$ \cdot (pink), (G4-H1) \cdot (blue) and (G4-H2) \cdot (green) in solid lines compared with that of G (dashed lines and same color code), PCM/TD-M052x/6-31G(d)//M052x/6-31G(d) calculations. The spectra are shifted by 0.6 eV.

2.2 Additional computational controls.

Due to the large size of G4, we made some approximations when computing the spectra, such as neglecting explicit water molecules, using a small basis set, and reducing the number of guanine residues into the QM part. However, we paid attention that all these ‘assumptions’ have negligible effect into the final outcomes of our calculations using the G monomer as benchmark. We also checked the robustness of our conclusion with respect to the choice of the functional, computing the spectra of the different radical bases using the

widely employed long-range corrected CAM-B3LYP¹⁰ functional. For simplicity, all the spectra showed below are not shifted on the energy scale.

Solvent effect

Inclusion of solvent either as a continuum or via explicit water molecules improves the agreement with the experiments, for what concerns especially intensity of the different peaks of (G)⁺• and (G4-H1)•, but has a very limited effect on the band position.

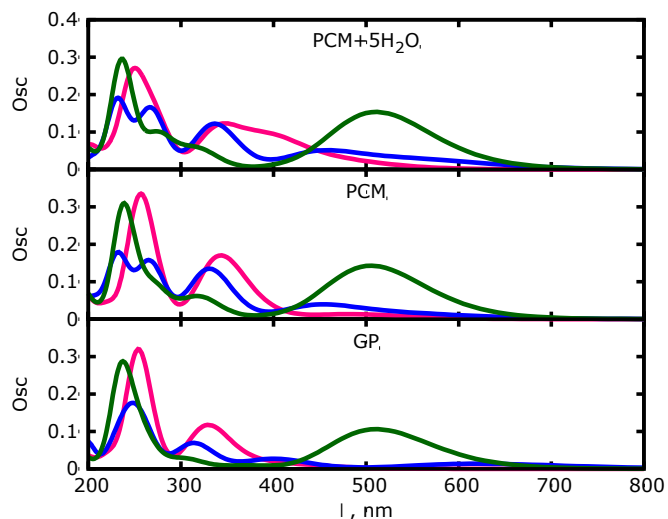


Figure S7. Computed absorption spectra for of (G)⁺• (pink), (G-H1)• (blue) and (G-H2)• (green) at the TD-M052x/6-31+G(d,p)//M052x/6-31G(d) level of theory, in the gas phase (GP) and in solution (PCM and PCM+5H₂O). Unshifted spectra.

Basis set effect

The influence of the basis set selected in both the geometry optimization and VAE calculations was also checked. The G geometry was optimized at the M052X/6-31+G(d,p) level of theory (in GP) and then the radicals spectra were calculated with different bases sets (Figure S8). It can be concluded that the increase of the basis set has a very limited effect on the position of the peaks, especially those in the red-wing. This result validates the use of the smaller basis set for G4 since a larger basis set would not affect dramatically the spectra of the radicals.

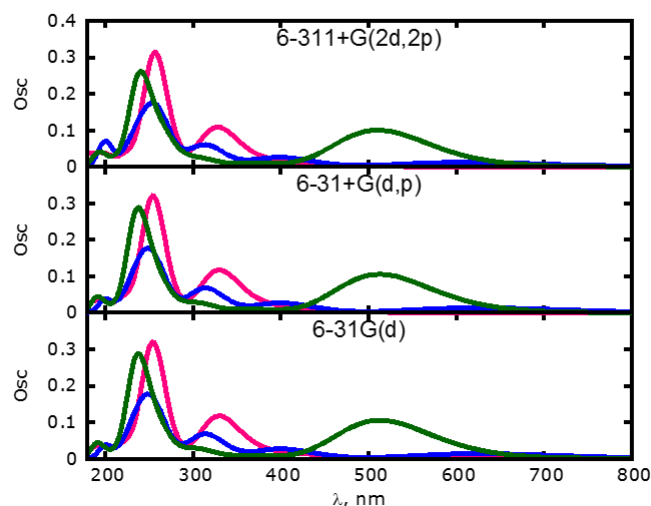


Figure S8. Computed absorption spectra for $(G)^{\bullet+}$ (pink), $(G-H1)^{\bullet}$ (blue) and $(G-H2)^{\bullet}$ (green) at the TD-M052x level of theory in the gas phase by using different basis sets.

Functional effect

We checked the dependence of our calculated spectra on the functional to verify if our conclusions are affected by the choice of M052X functional. We thus recomputed the radicals of the monomer with CAM-B3LYP functional. Both spectra are depicted in Figure S9. Although CAM-B3LYP is in slightly better agreement with the experimental spectra, both spectra are very similar, and since M052X is more suitable for geometry optimizations of stacked systems, we chose M052X to study G4.

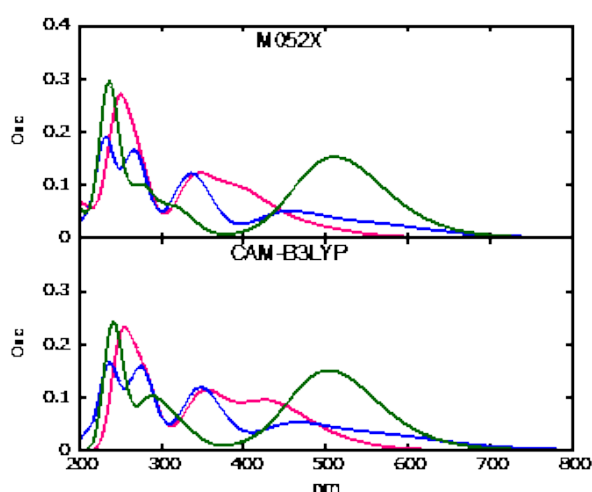


Figure S9. Computed absorption spectra for spectra for $G^{\bullet+}$ (pink), $(G-H1)^{\bullet}$ (blue) and $(G-H2)^{\bullet}$ (green) at the TD-M052x/6-31+G(d,p)//M052x/6-31G(d) and TD-CAM-B3LYP/6-31+G(d,p)//M052x/6-31G(d) levels of theory in PCM+5H₂O. Unshifted spectra.

Effect of the number of QM guanine bases on the absorption spectra

As already mentioned in the computational details, in order to cover the blue-wing of the spectrum it was necessary to decrease the number of bases considered at the QM level from 12 to 8. It is important to check if this further approximation affects the description of the red-wing of the radical spectra and if our 8-G model still recovers all the characteristic features of the G4 (neutral) absorption spectra. We compared the absorption of the radicals using the 8 and 12-model and as shown in Figure S10, the effect is very small. For the absorption of the neutral system we computed 90 excited states using both models and scaled the 12-model results by 0.67 (8/12) (to properly compare the relative intensities). Again, there is no change and all the significant features are recovered by the 8-model.

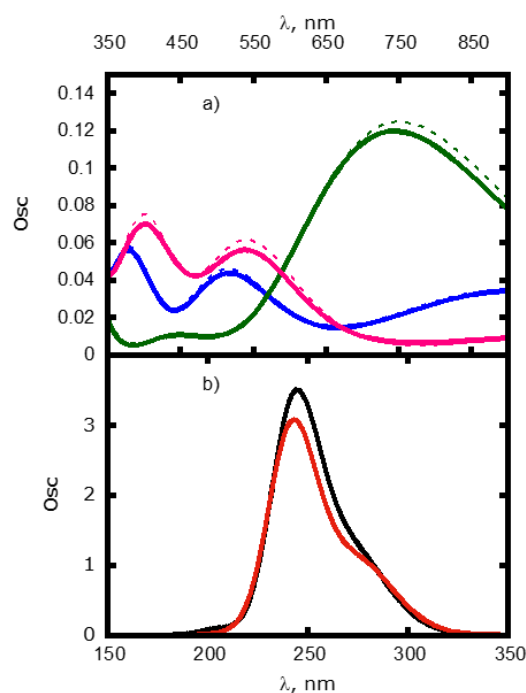


Figure S10. **a)** Simulated absorption spectra for G4⁺ (pink), (G4-H1)[•] (blue) and (G4-H2)[•] (green) for a different numbers of bases included in the QM region, 12 (solid lines) and 8 (dashed lines). PCM/TD-M052x/6-31G(d)//M052x/6-31G(d) calculations. **b)** Simulated absorption spectra for G4 including 12 QM bases (red) and 8 (black).

References

- (1) Candeias, L. P.; Steenken, S., *J. Am. Chem. Soc.* **1989**, *111*, 1094-1099.
- (2) Marguet, S.; Markovitsi, D., *J. Am. Chem. Soc.* **2005**, *127*, 5780-5781.
- (3) Zhao, Y.; Schultz, N. E.; Truhlar, D. G., *J. Chem. Theory Comput.* **2006**, *2*, 364-382.
- (4) Zhao, Y.; Truhlar, D. G., *Acc. Chem. Res.* **2008**, *41*, 157-167.
- (5) Miertus, S.; Scrocco, E.; Tomasi, J., *Chem. Phys.* **1981**, *55*, 117-129.
- (6) Tomasi, J.; Mennucci, B.; Cammi, R., *Chem. Rev.* **2005**, *105*, 2999-3093.
- (7) Cornell, W. D.; Cieplak, P.; Bayly, C. I.; Gould, I. R.; Merz, K. M.; Ferguson, D. M.; Spellmeyer, D. C.; Fox, T.; Caldwell, J. W.; Kollman, P. A., *J. Am. Chem. Soc.* **1995**, *117*, 5179-5197.
- (8) Dapprich, S.; Komaromi, I.; Byun, K. S.; Morokuma, K.; Frisch, M. J., *J. Mol. Struct.-Theochem* **1999**, *461*, 1-21.
- (9) Frisch, M. J.; Trucks, G. W.; Schlegel, H. B.; Scuseria, G. E.; Robb, M. A.; Cheeseman, J. R.; Scalmani, G.; Barone, V.; Mennucci, B.; Petersson, G. A.; Nakatsuji, H.; Caricato, M.; Li, X.; Hratchian, H. P.; Izmaylov, A. F.; Bloino, J.; Zheng, G.; Sonnenberg, J. L.; Hada, M.; Ehara, M.; Toyota, K.; Fukuda, R.; Hasegawa, J.; Ishida, M.; Nakajima, T.; Honda, Y.; Kitao, O.; Nakai, H.; Vreven, T.; Montgomery, J. A.; Peralta, J. J. E.; Ogliaro, F.; Bearpark, M.; Heyd, J. J.; Brothers, E.; Kudin, K. N.; Staroverov, V. N.; Kobayashi, R.; Normand, J.; Raghavachari, K.; Rendell, A.; Burant, J. C.; Iyengar, S. S.; Tomasi, J.; Cossi, M.; Rega, N.; Millam, J. M.; Klene, M.; Knox, J. E.; Cross, J. B.; Bakken, V.; Adamo, C.; Jaramillo, J.; Gomperts, R.; Stratmann, R. E.; Yazyev, O.; Austin, A. J.; Cammi, R. C.; Pomelli, C.; Ochterski, J. W.; Martin, R. L.; Morokuma, K.; Zakrzewski, V. G.; Voth, G. A.; Salvador, P.; Dannenberg, J. J.; Dapprich, S.; Daniels, A. D.; Farkas, O.; Foresman, J. B.; Ortiz, J. V.; Cioslowski, J.; Fox, D. J., *Gaussian 09, revision A.02*. Gaussian Inc.: Wallingford CT, 2009.
- (10) Yanai, T.; Tew, D. P.; Handy, N. C., *Chem. Phys. Lett.* **2004**, *393*, 51-57.